LEVEL

NPS-53-79-001

NAVAL POSTGRADUATE SCHOOL
Monterey, California

A TRANSFER FUNCTION ANALYSIS OF NUMERICAL SCHEMES

USED TO SIMULATE GEOSTROPHIC ADJUSTMENT
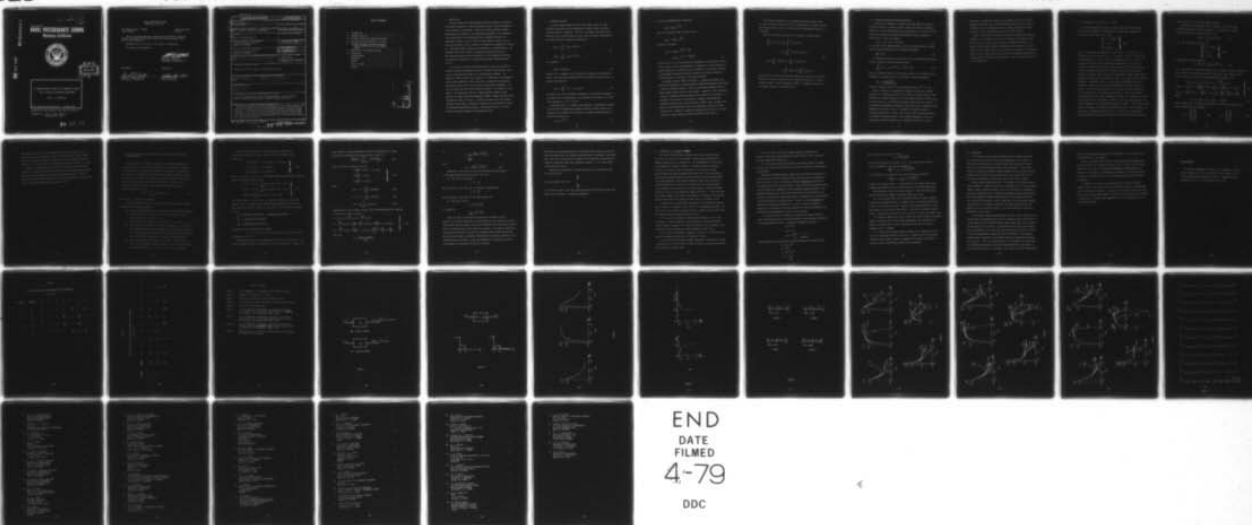
Arthur L. Schoenstadt

Final Report for Period January - October 1978

Approved for Public Release; Distribution Unlimited

Prepared for: Chief of Naval Research
Arlington, VA 22217

79 02 23 128
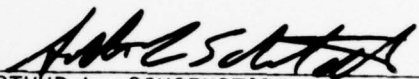
NAVAL POSTGRADUATE SCHOOL
Monterey, California

Rear Admiral Tyler F. Dedman   Jack R. Borsting
Superintendent   Provost

The work reported herein was supported by the Foundation Research
Program of the Naval Postgraduate School with funds provided by the
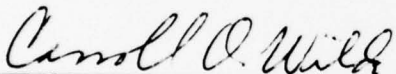Chief of Naval Research.

Reproduction of all or part of this report is authorized.
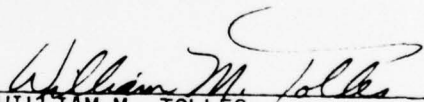
This report was prepared by:

ARTHUR L. SCHOENSTADT
Associate Professor
Department of Mathematics

Reviewed by: Released by:

CARROLL O. WILDE, Chairman   WILLIAM M. TOLLES
Department of Mathematics   Dean of Research

REPORT DOCUMENTATION PAGE		READ INSTRUCTIONS BEFORE COMPLETING FORM
1 REPORT NUMBER NPS-53-79-001	2. GOVT ACCESSION NO.	3. RECIPIENT'S CATALOG NUMBER
4. TITLE (and Subtitle) A TRANSFER FUNCTION ANALYSIS OF NUMERICAL SCHEMES USED TO SIMULATE GEOSTROPHIC ADJUSTMENT.		5. TYPE OF REPORT & PERIOD COVERED Final Jan - Oct 1978
		6. PERFORMING ORG. REPORT NUMBER
7. AUTHOR(s) Arthur L. Schoenstadt		8. CONTRACT OR GRANT NUMBER(s)
9. PERFORMING ORGANIZATION NAME AND ADDRESS Naval Postgraduate School Monterey, CA 93940		10. PROGRAM ELEMENT, PROJECT, TASK AREA & WORK UNIT NUMBERS 61152N, RR 000-01-01 N0001478WR80023
11. CONTROLLING OFFICE NAME AND ADDRESS Naval Postgraduate School Monterey, CA 93940		12. REPORT DATE November 1978
		13. NUMBER OF PAGES
14. MONITORING AGENCY NAME & ADDRESS(if different from Controlling Office) Final rept. Jan - Oct 78.		15. SECURITY CLASS. (of this report) UNCLASSIFIED
		15a. DECLASSIFICATION/DOWNGRADING SCHEDULE

16. DISTRIBUTION STATEMENT (of this Report)

Approved for Public Release; Distribution Unlimited

17. DISTRIBUTION STATEMENT (of the abstract entered in Block 20, if different from Report)

RR 00001   RR 0000101

18. SUPPLEMENTARY NOTES

48 p.

19. KEY WORDS (Continue on reverse side if necessary and identify by block number)

Finite Difference Methods, Finite Element Methods, Fourier Transform Analysis, Geostrophic Adjustment, Numerical Weather Prediction

20. ABSTRACT (Continue on reverse side if necessary and identify by block number)

Traditional analysis of finite difference and finite element schemes used in numerical weather prediction has concentrated almost exclusively on an analysis of the accuracy with which the scheme simulates the phase speeds involved. In this paper, we use the transfer function formulation common in design of electrical filters to show that these numerical schemes also have important amplitude distortion characteristics, which must be considered in any complete analysis.

DD FORM 1473 EDITION OF 1 NOV 65 IS OBSOLETE
1 JAN 73
S/N 0102-014-6601

TABLE OF CONTENTS

i

I. INTRODUCTION

The main concern when approximating either an ordinary or a partial differential equation by a discrete equation, either finite difference or finite element, is the degree to which the discrete equation solution approximates the solution to the differential equation. The closeness of this approximation has traditionally been considered from both its quantitative aspects, such as relative error (Henrici (1963)), and its qualitative aspects, such as behavior of transients, propagation of fronts, etc. (Haltiner (1971)). Analyses based primarily on consideration of the basically qualitative property of numerical dispersion, where the discretization process causes distortions in the propagation velocities for different frequencies, are especially prevalent (Arakawa and Lamb (1977)).

In this paper, we apply certain ideas derived from the concepts of transfer functions and digital filters in electrical engineering to the study of the qualitative behavior of discretization schemes. The particular model we shall use is based on the linearized, one dimensional shallow water equations, without mean flow, a model which has important application to the study of the process of geostrophic adjustment. (It will be evident that the basic approach, however, is not limited to this model.) The qualitative effects of discretization schemes on this equation have been studied by Winninghoff (1968), Arakawa and Lamb (1977), Schoenstadt (1977), and others. We shall show that use of the transfer function concept leads to important insights into the differences caused by different discretization schemes - differences that are not fully evident from phase propagation considerations only.

-1-

II. TRANSFER FUNCTIONS

It is well known (Stremler (1977)) that linear, space (or time) invariant systems can be fully described in terms of their so-called transfer function. (Figure 1) That is, if we denote the input to the system as $y_i(x)$, and the output as $y_o(x)$, then the Fourier transforms of the input and output, denoted respectively as

$$\tilde{y}_i(k) = \int_{-\infty}^{\infty} y_i(x) \, e^{-ikx} \, dx \quad ,$$

$$\tilde{y}_o(k) = \int_{-\infty}^{\infty} y_o(x) \, e^{-ikx} \, dx \quad ,$$

(1)

are related by

$$\tilde{y}_o(k) = \tilde{\phi}(k)\tilde{y}_i(k) \quad . \tag{2}$$

Equation (2) is commonly said to represent the system in the transform domain. The equivalent representation in the physical (time or space, as appropriate) domain is

$$y_o(x) = \int_{-\infty}^{\infty} \phi(x - s) \, y_i(s) \, ds \quad . \tag{3}$$

In equation (3), $\phi(x)$ is commonly referred to as the impulse response of the system, and is interpreted as the response of the system to an input delta function at $x = 0$, i.e. $\delta(x)$.

In general, $\tilde{\phi}(k)$ is a complex valued function. The physical interpretation of both the magnitude and phase of $\tilde{\phi}(k)$ is easily arrived at by considering the response of the system to a single sinusoidal input of arbitrary frequency, i.e.

$$y_i(x) = e^{ik_i x} \quad . \tag{4}$$

-2-

It is very straightforward to show that

$$y_o(x) = \overset{\vee}{\phi}(k_i) \, e^{ik_i x} \quad .$$

Thus, if we represent $\overset{\vee}{\phi}(k)$ in polar form as

$$\overset{\vee}{\phi}(k_i) = |\overset{\vee}{\phi}(k_i)| \, e^{ik_\phi} \quad ,$$

equation (5) becomes:

$$y_o(x) = |\overset{\vee}{\phi}(k_i)| \, e^{i(k_i x + k_\phi)} \quad ,$$

$$= |\overset{\vee}{\phi}(k_i)| \, e^{ik_i(x + (k_\phi/k_i))} \quad . \tag{5}$$

Clearly, from (5), we can interpret the magnitude of the transfer function as the factor by which the amplitude of a sinusoid of a given frequency is either amplified or attenuated, and the argument of the transfer function as determining the amount by which the phase of the output sinusoid is shifted relative to the phase of the input sinusoid.

In general, neither $|\overset{\vee}{\phi}(k)|$ nor (k_ϕ/k) is constant, and hence, the different frequencies in a given input are amplified/attenuated and shifted in phase by different amounts. Thus the output signal generally has its shape (graph) altered from the input signal. (Figure 2) This alteration of shape is commonly called distortion, and, based on our discussion, is composed of the effects of _two_ actions – commonly called amplitude distortion, which is due to the deviation of $|\overset{\vee}{\phi}(k)|$ from a constant, and phase (or delay) distortion, due to the deviation of k_ϕ from a linear function of k. Clearly, to completely understand the effect of a linear system on an input signal, one must know both of these effects.

-3-

In electrical engineering, it is common to call any linear, time (or space) invariant device, which can be described by a transfer function as discussed above, a filter. We shall use the terminology hereafter in this paper.

Lastly we note that the energy in an "output" is proportional to

$$\int_{-\infty}^{\infty} y_o^{\,2}(x) \; dx = \frac{1}{2\pi} \int_{-\infty}^{\infty} |\tilde{y}_o(k)|^2 \; dk \quad ,$$

$$= \frac{1}{2\pi} \int_{-\infty}^{\infty} |\tilde{\phi}(k) \; \tilde{y}_i(k)|^2 \; dk$$

$$\leq \frac{1}{2\pi} \{ \int_{-\infty}^{\infty} |\tilde{\phi}(k)|^2 \; dk \} \{ \int_{-\infty}^{\infty} |y_i(k)|^2 \; dk \} \quad , \tag{6}$$

$$= \{ \int_{-\infty}^{\infty} |\tilde{\phi}(k)|^2 \; dk \} \int_{-\infty}^{\infty} y_i^{\,2}(x) \; dx$$

and thus one can also use the transfer function to describe the relation between the energies contained in the "input" and "output" to a linear, invariant system. (Note the quantity $|\tilde{y}(k)|^2$ is commonly referred to as the spectral density of the signal $y(x)$.)

III. DISCRETE FILTERS AND TRANSFER FUNCTIONS

A great deal of research is presently directed toward the study of so-called discrete, or digital filters, which arise when the continuous processes, such as differentiation and integration, in an invariant linear filter are replaced by analogous approximations based on sampled, or discrete data. Thus, for example,

$$y(x + \Delta x) = y(x) + f(x) (\Delta x) \quad , \tag{7}$$

is a digital filter approximating, in some sense (specifically by using an Euler forward predictor), the continuous integrator:

$$\frac{dy}{dx} = f(x) \quad . \tag{8}$$

The transfer functions of such filters can be easily determined using Fourier transforms, and the observation that

$$\int_{-\infty}^{\infty} y(x + \Delta x) \, e^{-ikx} \, dx = e^{ik(\Delta x)} \, \tilde{y}(k) \quad . \tag{9}$$

Thus, the transfer function of the process given by (7) is (where $f(x)$ is considered the "input" and $y(x)$ the "output"), after some algebra,

$$\overset{\sim}{\phi}(k) = \frac{(\Delta x) e^{ik(\Delta x)/2}}{2i \, \sin(k(\Delta x)/2)} \quad .$$

(Note the transfer function of the continuous process is $\overset{\sim}{\phi}{}^{c}(k) = \frac{1}{ik}$.)

There is, however, one significant difference between the transfer functions of a continuous filter and its digital (discrete) analog. This difference is commonly referred to with the terms aliasing or folding, and the basic work on it is commonly attributed to Nyquist (Clark (1977)). In its simplest interpretation, Nyquist's work implies that a sampling device, sampling at intervals of (Δx), is incapable of resolving waves of frequency greater than ($\pi/(\Delta x)$), and, if any energy is actually present in a sampled continuous signal at these higher frequencies, it will be erroneously resolved (aliased) into a frequency lower than ($\pi/(\Delta x)$).

-5-

Thus, while a continuous filter can, in principle, react to any input frequency, and hence has a transfer function defined for all k, that of a digital filter is considered only for (complex) frequencies between $\pm(\pi/(\Delta x))$, the so-called Nyquist cut-off or Nyquist limit.

Lastly, we note that if a digital filter has a significant amplitude response (i.e. if $|\overset{\sim}{\phi}(k)|$ is not close to zero) near the Nyquist limit, then the output of that system may have a significant portion of its energy in these high frequency oscillations. These oscillations often appear to the observer as noise, or "noise-like", and hence, in discussing digital filter design, many books and articles recommend controlling the transfer function response near this limit. (This is sometimes referred to as "windowing".)

IV. THE SHALLOW WATER EQUATIONS AS A FILTER

The basic equations we propose to study, using the ideas discussed above, are the linearized, one-dimensional, shallow water equations in an infinite region, with no mean flow:

$$\left.\begin{aligned}
\frac{\partial u}{\partial t} - fv + g\,\frac{\partial h}{\partial x} &= 0 \\[6pt]
\frac{\partial v}{\partial t} + fu &= 0 \\[6pt]
\frac{\partial h}{\partial t} + H\,\frac{\partial u}{\partial x} &= 0 \,,
\end{aligned}\right\} \qquad (10)$$

where u denotes the perturbation velocity in the x direction, v the perturbation velocity normal to the x direction, H and h the mean and perturbed heights of the free surface, respectively, and $g > 0$ and $f > 0$ the gravitational and Coriolis parameters, respectively. This model is especially important in the study of the meteorological process called geostrophic adjustment, which has been studied in some detail from several approaches by Rossby (1937), Cahn (1945), Winninghoff (1968), Blumen (1972), Arakawa and Lamb (1977) and Schoenstadt (1977). This process of geostrophic adjustment is important because it is the primary mechanism by which an atmosphere, modeled by the so-called meteorological primitive equations, reacts to errors (either numerical or due to errors in observational data) in the initial data. The dispersive wave nature of (10) is the primary mechanism by which these errors (commonly referred to as "imbalances") eventually spread out over the domain of interest, until the system reaches a so-called "balanced" or "geostrophically adjusted" condition. Forecasts at times before this balance is reached are generally inaccurate. Thus a primary consideration in numerically modeling (10) is to insure that the numerical balance mechanism both fairly accurately models the physical balancing pro-

-7-

cedure, and that it proceeds relatively quickly.

As discussed in Schoenstadt (1977), equations (10) can be easily
solved by using spatial Fourier transform. If we continue to denote
Fourier transforms by an overhead tilde, e.g.:

$$\tilde{u}(k,t) = \int_{-\infty}^{\infty} u(x,t) e^{-ikx} \, dx \; , \qquad (11)$$

etc. Then (10) reduces directly to:

$$\left. \begin{aligned} \frac{d\tilde{u}}{dt} &= f\tilde{v} - ikg \, \tilde{h} \; , \\ \frac{d\tilde{v}}{dt} &= -f \, \tilde{u} \; , \\ \frac{d\tilde{h}}{dt} &= -ik \, H \, \tilde{u} \; , \end{aligned} \right\} \qquad (12)$$

together with initial conditions:

$$\tilde{u}_i = \tilde{u}(k,0) = \int_{-\infty}^{\infty} u(x,0) e^{-ikx} \, dx \; , \qquad (13)$$

etc. Then since (12) represents simply a set of coupled, constant coefficient
(in the sense of t) ordinary differential equations, their solution can be
easily shown, by the usual eigenvalue/eigenvector approach, to be:

$$\left. \begin{aligned} \tilde{u}(k,t) &= \tilde{u}_i \cos \nu t + \frac{f \, \tilde{v}_i}{\nu} \sin \nu t - \frac{ikg \, \tilde{h}_i}{\nu} \sin \nu t \; , \\ \tilde{v}(k,t) &= - \frac{f}{\nu} \tilde{u}_i \sin \nu t + \left\{ \frac{k^2 gH}{\nu^2} + \frac{f^2}{\nu^2} \cos \nu t \right\} \tilde{v}_i + \frac{ikgf}{\nu^2} \left\{ 1 - \cos \nu t \right\} \tilde{h}_i \; , \\ \tilde{h}(k,t) &= - \frac{ikH}{\nu} \tilde{u}_i \sin \nu t - \frac{ikHf}{\nu^2} \left\{ 1 - \cos \nu t \right\} \tilde{v}_i + \left\{ \frac{f^2}{\nu^2} + \frac{k^2 gH}{\nu^2} \cos \nu t \right\} \tilde{h}_i \end{aligned} \right\} \qquad (14)$$

where:

$$\nu^2 = f^2 + k^2 gH = f^2 (1 + \lambda^2 k^2), \quad \lambda = \sqrt{gH}/f \; . \qquad (15)$$

We now consider (14) in view of our discussion of filters and transfer func-
tions. Observe that if we denote

$$\underline{y}_i = \begin{bmatrix} u_i \\ v_i \\ h_i \end{bmatrix} \qquad \text{and} \qquad \underline{y}_0 = \begin{bmatrix} u \\ v \\ h \end{bmatrix} \qquad (16)$$

-8-

respectively, as the "input" and "output" to the "system" described by (10), then we can express (14) as

$$\tilde{\underline{y}}_o = \tilde{\underline{\underline{\phi}}}(k,t)\tilde{\underline{y}}_i \qquad (17)$$

where,

$$\tilde{\underline{\underline{\phi}}}(k,t) = \begin{bmatrix} \cos \nu t & \dfrac{f_o}{\nu} \sin \nu t & \dfrac{ikg_o}{\nu} \sin \nu t \\[3mm] -\dfrac{f}{\nu} \sin \nu t & \left\{ \dfrac{k^2 gH}{\nu^2} + \dfrac{f^2}{\nu^2} \cos \nu t \right\} & \dfrac{ikgf}{\nu^2} \{1 - \cos \nu t\} \\[3mm] -\dfrac{ikH}{\nu} \sin \nu t & -\dfrac{ikHf}{\nu^2} \{1 - \cos \nu t\} & \left\{ \dfrac{f^2}{\nu^2} + \dfrac{k^2 gH}{\nu^2} \cos \nu t \right\} \end{bmatrix} \qquad (18)$$

Immediate comparison of (17)-(18) with (2) is not possible since $\tilde{\underline{\underline{\phi}}}(k,t)$ depends not only on the transform variable ("k"), but also on one of the physical variables ("t"). However, since $\sin \nu t$ and $\cos \nu t$ can be expressed in terms of $e^{\pm i\nu t}$, and since k is real, it is easily seen that the sinusoidal terms in (18) express only the phase relationships (which clearly change with time), while the other, time independent, coefficients reflect the amplitude effects of the "filter". In fact, it is fairly easy to show (Schoenstadt (1977)) that the sinusoidal terms in (18) produce dispersive, transient waves, propagating throughout the region. (These waves are clearly dispersive since $(\nu(k)/k)$ is not constant.) The *time independent coefficients* in (18) still function as amplitude distortion terms in the sense that they redistribute the energy that is in the input (initial condition) waves, in a manner that varies with wave number, into the output (solution) waves.

A close examination of (18) shows that, in fact, the "amplitude distortion" in this "system" is really governed in each term by precisely one of

-9-

the three factors,

$$\frac{1}{\nu} \, , \qquad \frac{k}{\nu} \qquad \text{or} \qquad \frac{k}{\nu^2} \, ,$$

or the square of one of these. The amplitude response curves for these three expressions are shown in Figure 3. It is clear that the terms with the coefficient $(1/\nu)$ have their low frequencies least affected, the terms with coefficient (k/ν) their high frequencies least affected, and those with coefficient (k/ν^2) their frequencies in some middle range least effected. Such responses are often referred, respectively, to as low pass, high pass, and band pass filters.

Since the "system" described by (10) involves both spatial and temporal variation, it is well known that not only the phase velocity $(\nu(k)/k)$, but also the group velocity $(\frac{d\nu}{dk})$ is important in describing the behavior, since it is the latter which governs the rate at which energy actually propagates. Thus, in Figure 4, we display both of these velocities for the system (10).

We note that additional insight into some of the qualitative behavior of the solution to (10) can be obtained by decomposing (18) into its transient and steady state components, i.e., writing

$$\underset{\sim}{\tilde{y}}_o = \underset{\approx}{\tilde{\phi}}_S \, \underset{\sim}{\tilde{y}}_i + \underset{\approx}{\tilde{\phi}}_T \, \underset{\sim}{\tilde{y}}_i \, , \qquad (19)$$

where $\underset{\approx}{\tilde{\phi}}_S$ and $\underset{\approx}{\tilde{\phi}}_T$ can be obtained by inspection, since only time dependent terms contribute to the transients, however, we shall not pursue this analysis here.

As a final comment, note that the total energy of the system represented by (10) is given by:

$$u^2 + v^2 + \frac{g}{H} h^2 \, .$$

Thus the spectral density of the steady state field can be shown to be

$$|u_S|^2 + |v_S|^2 + \frac{g}{H} |h_S|^2 = \frac{gHk^2}{\nu^2} |v_i|^2 + \frac{gf^2}{H\nu^2} |h_i|^2 \, . \qquad (20)$$

-10-

Since the term (k/ν) acts as a high-pass filter, and the term (f/ν) as a low pass-filter, we see that the energy in the steady state field is determined by a combination depending primarily on the high frequency energy in the initial v field, and the low frequency energy in the initial h field.

We shall not proceed any further with this analysis, since our main interest is to analyze how discrete schemes, and the corresponding "filters" they produce, approximate the continuous (differential) model. However, there are certainly other insights into the general behavior of the physical model still possible from this filter point of view.

V. TRANSFER FUNCTIONS FOR QUASI-DISCRETE FINITE DIFFERENCE AND FINITE
    ELEMENT METHODS

In this section, we extend the analysis of our continuous model to
the quasi-discrete case, where continuous spatial operations are replaced
by operations only at sample points, while the continuous time operations
are retained. This approach follows that in Winninghoff (1968) and Arakawa
and Lamb (1977). However, we extend our analysis to include a more general
case of quasi-discrete schemes than they considered. Specifically, we
define an invariant linear discretization operator about the point x as
any operator having the form

$$L[f(x)] = \sum_{n=-n_1}^{n_2} c_n f(x + n(\Delta x)) ,$$ (21)

where the c_n denote real constants.

The discretization schemes we shall investigate are specifically those
satisfying the following conditions:

(a) All discretization operators are linear and time and space invariant.

(b) All discretization operators operate only on symmetric sets of
     sample points, i.e. in (21), $n_1 = n_2$.

(c) The discretization operators are balanced, i.e. in (21) $|c_n| = |c_{-n}|$.

(d) The operators are applied to (3)-(10) consistently, i.e. if one of
     the derivative terms on the right hand side of (8)-(10) is replaced
     by a certain difference, then all derivative terms on the right hand
     side of (8)-(10) are replaced by the same difference operator.

(e) The discretization must be exact, i.e. produce exactly the same
     result as the analogous continuous operation, on all at least arbi-
     trary linear functions, i.e. $f(x) = ax + b$, a, b, arbitrary.

-12-

With these restrictions, it is fairly simple to show that the quasi-discrete schemes we wish to consider can all be reduced to the general form:

$$\frac{\partial}{\partial t} \{L_\alpha[u(x,t)]\} = f\, L_\beta[v(x,t)] - g\, L_\sigma[h(x,t)]$$

$$\frac{\partial}{\partial t} \{L_\alpha[v(x,t)]\} = -f\, L_\beta[u(x,t)] \qquad\qquad (22)$$

$$\frac{\partial}{\partial t} \{L_\alpha[h(x,t)]\} = -H\, L_\sigma[u(x,t)]$$

where $L_\alpha[\ ]$, $L_\beta[\ ]$, and $L_\sigma[\ ]$, are invariant linear discretization operators having the following general form:

$$L_\alpha[f(x)] = \alpha_o f(x) + \sum_{n=1}^{n_\alpha} \alpha_n[f(x + n\Delta x) + f(x - n\Delta x)]$$

$$L_\beta[f(x)] = \beta_o f(x) + \sum_{n=1}^{n_\beta} \beta_n[f(x + n\Delta x) + f(x - n\Delta x)] \qquad (23)$$

$$L_\sigma[f(x)] = \frac{1}{\Delta x} \sum_{n=1}^{n_\sigma} \sigma_n[f(x + n\Delta x) - f(x - n\Delta x)]$$

The various values of α_n, β_n, and σ_n will be referred to as the filter weights. Thus, for example, the finite difference mesh which Arakawa and Lamb (1977) call Scheme C (Figure 5), and which is given in finite difference form as

$$\frac{\partial u}{\partial t} = f\frac{v(x+d/2,t) + v(x-d/2,t)}{2} - g\frac{h(x+d/2,t) - h(x-d/2,t)}{d}$$

$$\frac{\partial v}{\partial t} = -f\frac{u(x+d/2,t) + v(x-d/2,t)}{2}$$

$$\frac{\partial h}{\partial t} = -H\frac{u(x+d/2,t) - u(x-d/2,t)}{d}$$

corresponds to the following filter weights:

$$\alpha_o = 1, \ \beta_1 = \frac{1}{2}, \ \sigma_1 = \frac{1}{2}, \ \text{all others zero.} \quad \text{(Note that in this}$$

formulation $\Delta x = d/2$.)

Determination of the filter properties of the system represented by (22) requires taking the Fourier transform (in x) of those equations. However, the

-13-

shift property of these transforms (equation (9)) simplifies the terms
involving the discretization operators, since, using (9)

$$\widetilde{\{L[f(x)]\}} = \left\{ \sum_{n=-n_1}^{n_2} c_n \, e^{ikn(\Delta x)} \right\} \tilde{f}(k) \ . \tag{24}$$

Thus, the Fourier transform of (22) is

$$\alpha(k)\frac{d\tilde{u}}{dt} = f \, \beta(k)\tilde{v} - i \, g \, \sigma(k)\tilde{h} \ ,$$

$$\alpha(k)\frac{d\tilde{v}}{dt} = -f \, \beta(k)\tilde{u} \ , \qquad\qquad \left.\right\} \tag{25}$$

$$\alpha(k)\frac{d\tilde{h}}{dt} = -i \, H\sigma(k)\tilde{u} \ ,$$

where

$$\alpha(k) = \alpha_o + 2 \sum_{n=1}^{n_\alpha} \alpha_n \cos(nk\Delta x) \ , \tag{26}$$

$$\beta(k) = \beta_o + 2 \sum_{n=1}^{n_\beta} \beta_n \cos(nk\Delta x) \ , \tag{27}$$

$$\sigma(k) = \frac{2}{\Delta x} \sum_{n=1}^{n_\sigma} \sigma_n \sin(nk\Delta x) \ . \tag{28}$$

Equations (25) can be solved, using the same eigenvalue/eigenvector approach
as was used for (12), to yield:

$$\tilde{u} = \tilde{u}_o \cos \hat{\nu}t + \frac{f\beta\tilde{v}_o}{\nu} \sin \hat{\nu}t - \frac{i\sigma g\tilde{h}_o}{\nu} \sin \hat{\nu}t$$

$$\tilde{v} = -\frac{f\beta\tilde{u}_o}{\nu} \sin \hat{\nu}t + \left\{ \frac{\sigma^2 gH}{\nu^2} + \frac{f^2\beta^2}{\nu^2} \cos \hat{\nu}t \right\}\tilde{v}_o + \frac{i\sigma gf\beta}{\nu^2} \{1 - \cos \hat{\nu}t\}\tilde{h}_o \qquad \left.\right\} \tag{29}$$

$$\tilde{h} = -\frac{i\sigma H\tilde{u}_o}{\nu} \sin \hat{\nu}t - \frac{i\sigma Hf\beta}{\nu^2}\{1 - \cos \hat{\nu}t\}\tilde{v}_o + \left\{ \frac{f^2\beta^2}{\nu^2} + \frac{\sigma^2 gH}{\nu^2} \cos \hat{\nu}t \right\}\tilde{h}_o$$

where now

$$\hat{\nu}^2 = \frac{f^2\beta^2(k) + gH\sigma^2(k)}{\alpha^2(k)} \ ,$$

-14-

or

$$\hat{v} = \frac{f}{\alpha(k)} \sqrt{\beta^2(k) + \lambda^2\sigma^2(k)}, \qquad (30)$$

$$= \frac{\nu(k)}{\alpha(k)},$$

where

$$\nu(k) = f\sqrt{\beta^2(k) + \lambda^2\sigma^2(k)} . \qquad (31)$$

Comparison of (29)-(31) with (14)-(15) show that the main impacts of the quasi-discretization described by (22) are:

(1) The filter coefficients

$$\frac{1}{\nu} , \frac{k}{\nu} , \frac{k}{\nu^2}$$

and the squares of the first two, are replaced, respectively,

$$\frac{\beta}{\nu} , \frac{\sigma}{\nu} , \frac{\beta\sigma}{\nu^2}$$

and the squares of the first two of these expressions.

(2) The phase velocity

$$\frac{\nu}{k} = \frac{f}{k} \sqrt{1 + \lambda^2 k^2}$$

is replaced by

$$\frac{f}{k\alpha(k)} \sqrt{\beta^2 + \lambda^2\sigma^2} .$$

Since the filter coefficients discussed above determine how the energy in the initial disturbance is partitioned into the transient and steady state fields, then the degree to which the discrete filter coefficients approximate the continuous ones can be viewed as a measure of the degree to which the discretization accurately protrays the continuous model energy distribution. Any difference between a continuous (differential) coefficient, and the corresponding discrete coefficient, should be considered as introducing a distortion between the continuous and discrete solutions.

-15-

Similarly, any differences between the continuous phase and group velocities
and the discrete ones will result in distortion due to spreading of the waves.
This effect will be especially noticeable if the distortion is pronounced at
(spatial) frequencies that carry significant energy, i.e. for which filter
coefficients are "large".

Actually, as noted before, the phase velocity is less important than
the group velocity,

$$\frac{d\nu}{dk}$$

in the continuous case, and

$$\frac{d\hat{\nu}}{dk}$$

in the discrete case, since this quantity measures the velocity at which the
energy in the different frequencies propagates.

VI. COMPARISON OF THE ARAKAWA SCHEMES

The specific discretization schemes which we shall analyze using
(22)-(30) are based on the arrangements of sample points described in
Arakawa and Lamb (1977) as Schemes A-D. The arrangements of these points
in one dimension is shown is Figure 5. We shall consider both finite
difference and finite element formulations of the discrete problem,
whereas Arakawa and Lamb considered only second order finite differences.
The finite difference formulations are derived for both second and fourth
order approximations to the spatial derivative terms, while the finite
element formulations are derived (for Schemes A-C only) using piecewise
linear elements (the so-called "hat" function basis). The filter weights
derived for each of these methods are shown in Tables 1-3. Note that since
each scheme "samples" the initial disturbances at a distance of d, then the
shortest wave that can be resolved in each case is of frequency (π/d).

In Figures 6-8, the amplitude coefficients of the discretized approxi-
mate "filters" are compared to the "filters" in the differential model, for
the values of the physical parameters given in Arakawa and Lamb (1977). The
following qualitative generalizations are clear:

(1) In each of the methods (second order difference, fourth order
difference, or finite elements), the arrangement of points specified by
Scheme A appears to produce the greatest distortion, and, furthermore, this
distortion is most pronounced at high frequencies (short waves).

(2) In each of the methods, Schemes B, C and D very accurately approx-
imate the transfer function for the "high pass" filter.

(3) In each of the methods, Scheme C understates the amount of energy
distributed into the short waves by both the low-pass and band pass filters,
while Scheme B overstates this.

-17-

(4) In all cases, the finite element formulation appears more "accurate" than fourth order differences, which in turn is more "accurate" than the second order differences.

(5) The (group) velocity distortion is especially serious in Schemes A and D, since for short waves there is actually a reversal in the direction of propagation.

Note that even though Scheme B seems to have the least "distortion" in each case, there is still significant phase and group velocity distortion near the cut-off. Thus, we should not conclude immediately that Scheme B will produce the least "noisy" solutions. This is because the apparent noise in the solution is a combination of both amplitude and phase behavior, and any phase distortion may lead to perceived "noise" in the solution if (as is the case in Scheme B) significant energy is retained (due to the amplitude distortion effects) in the short waves. In fact, it may be preferable to tolerate more amplitude distortion, if it acts to reduce the amount of energy in the short waves, which are generally the slowest propagating, and which produce the appearance of noise in the solutions.

As a final check on our analysis, we compared the height fields for both the continuous and all the discrete models, using the same methodology as in Arakawa and Lamb (1977). An initial disturbance given by:

$$u_i(x,0) = 0$$

$$h_i(x,0) = 0$$

$$v_i(x,0) = \begin{cases} v_0 & , \ -a < x < a \\ 0 & , \ \text{otherwise} \end{cases}$$

was considered, with the physical parameters having the following values

$$g = 10 \ m \ sec^{-2}$$

$$H = 10^3 \ m$$

$$f = 10^{-4} \ sec^{-1}$$

$$a = d = \lambda/2.$$

-18-

The transform of the initial v field

$$\tilde{v}_i = \frac{2V_0 \sin(ka)}{k}$$

was then band limited to the region $-\frac{\pi}{d} < k < \frac{\pi}{d}$, and the exact solution

for h was computed as the inverse transform of

$$-\frac{ikHf}{\nu^2} \{1 - \cos \nu t\}\{\frac{2V_0 \sin(ka)}{k}\}$$

in the continuous (differential) case, and the inverse transform of

$$-\frac{i\sigma\beta fH}{\nu^2} \{1 - \cos(\frac{\nu}{\alpha} t)\}\{\frac{2V_0 \sin(ka)}{k}\}$$

in each of the discrete cases. In each instance, the inversion was accomplished using Simpson's rule on the interval $(0, \frac{\pi}{d})$, with 600 subintervals.

The different h fields are shown at Figure 9. Note that these agree with our predictions, based on the filter analysis, in that:

(1) In the second order finite difference methods, Scheme A displays a great deal of numerical noise, as predicted due to the great amplitude distortion of its filter near (π/d). Schemes B and D show somewhat less noise than Scheme A, but still more than Scheme C, this due to the manner in which Scheme C controls the amplitude near (π/d) in both the (σ/ν) and $(\beta\sigma/\nu^2)$ terms.

(2) Similar comments hold for the fourth order finite difference methods, though, in general, due to better phase propagation, the spreading of the energy in the short waves is not so pronounced, and hence the noise in Schemes B and D is reduced.

(3) In the finite element methods, Scheme A still remains quite noisy, due to its amplitude distortion near (π/d). Schemes B and C are virtually identical, since Scheme B seems to compensate for slightly more energy in the short waves by maintaining better phase relationship.

-19-

VII CONCLUSIONS

In this paper we have adapted concepts that are commonly associated with the design of filters in electrical engineering to the analysis of discretized representations of partial differential equations, and specifically to the one dimensional shallow water equations. We have shown that these concepts can provide valuable insights into why certain solution schemes provide "better" solutions than other, and a useful tool for comparing both qualitative and quantative aspects of different schemes.

We have clearly demonstrated that, in contrast to the analysis used in earlier studies, a complete analysis of the suitability of a certain discrete scheme to model a physical process, in our case the process of geostrophic adjustment, depends not only on providing reasonably accurate duplication of the phase propagation (delay) characteristics of the modeled system, but also on producing reasonably accurate duplication of the amplitude response characteristics. Furthermore, because of the phase distortion near the Nyquist cut-off of discrete schemes, it is often desirable to control the amplitudes of short waves.

In the process of geostrophic adjustment studies, we have concluded that schemes that use unstaggered grid points are generally poor, irrespective of the particular finite difference/finite element method used, due to some inherent properties of the model. The difficulties which have been reported with these methods in the literature, and especially the problem of "noise" in finite element models, appears directly attributable to the amplitude response near the Nyquist cut-off methods based on an unstaggered arrangement of points. This is certainly related to the tendency of schemes based on unstaggered grid points to produce solution separation, and appears to arise from the fact that the coupling of the fields in the basic differential

-20-

equation simply makes specifying all the quantities at every grid point an overspecification of the problem.

Lastly, we conclude, that, based on the one dimensional evidence only, the method identified by Arakawa and Lamb (1977) as Scheme C has been quite popular, not only due to its good phase propagation characteristics, but also due to its tendency, in either finite difference or finite element formulations, to "window" out much of the high frequency noise in the discretized model.

In summary, the concepts we have applied yield extremely valuable insights into the qualitative behavior of discrete methods for approximating partial differential equations. In many ways, we have only started to bring much of the emerging understanding of digital filters to bear on this problem. A significant, and interesting outgrowth will be the consideration of two dimensional problems.

ACKNOWLEDGMENTS

-22-

REFERENCES

Arakawa, A. and Lamb, V. R., "Computational Design of the Basic Dynamical Processes of the UCLA General Circulation Model", Methods of Computational Physics, Vol. 17, Academic Press, 1977.

Blumen, W., "Geostrophic Adjustment," Reviews of Geophysics and Space Physics, Vol. 10, No. 2, May 1972, pp. 485-528.

Cahn, A., "An Investigation of the Free Oscillations of a Simple Current System," Journal of Meteorology, Vol. 2, No. 2, 1945, pp. 113-119.

Clark, A. P., Advanced Data Transmission Systems, Halsted Press (Wiley), 1977.

Haltiner, G. J., Numerical Weather Prediction, John Wiley and Sons, Inc., 1971.

Henrici, P., Error Propagation for Finite Difference Methods, John Wiley and Sons, Inc., 1963.

Rossby, C. G., "On the Mutual Adjustment of Pressure and Velocity Distributions in Certain Simple Current Systems," J. Mar. Res., 1, 1937-1938, pp. 15-28, 239-263.

Schoenstadt, A., "The Effect of Spatial Discretization on the Steady-State and Transient Behavior of a Dispersive Wave Equation," J. Comp. Phys., Vol. 23, April 1977, pp. 364-379.

Stremler, F. G., Introduction to Communication Systems, Addison-Wesley, 1977.

Winninghoff, F., "On the Adjustment Toward a Geostrophic Balance in a Simple Primitive Equation Model with Application to the Problem on Initialization and Objective Analysis," Doctoral Dissertation, UCLA, 1968.

TABLE 1

FILTER WEIGHTS FOR SECOND ORDER FINITE DIFFERENCES

$$(\Delta x = d/2)$$

SCHEME	DENOTED	α_o	β_o	β_1	σ_1	σ_2
A	A2	1	1	0	0	$\frac{1}{4}$
B	B2	1	1	0	$\frac{1}{2}$	0
C	C2	1	0	$\frac{1}{2}$	$\frac{1}{2}$	0
D	D2	1	0	$\frac{1}{2}$	0	$\frac{1}{4}$

TABLE 2

FILTER WEIGHTS FOR FOURTH ORDER FINITE DIFFERENCES

$(\Delta x = d/2)$

SCHEME	DENOTED	α_0	β_0	β_1	σ_1	σ_2	σ_3	σ_4
A	A4	1	1	0	0	$\frac{8}{24}$	0	$-\frac{1}{24}$
B	B4	1	1	0	$\frac{27}{48}$	0	$-\frac{1}{48}$	0
C	C4	1	0	$\frac{1}{2}$	$\frac{27}{48}$	0	$-\frac{1}{48}$	0
D	D4	1	0	$\frac{1}{2}$	0	$\frac{8}{24}$	0	$-\frac{1}{24}$

TABLE 3

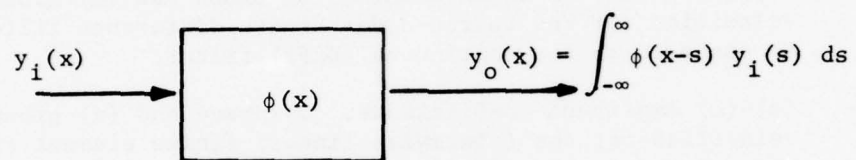FILTER WEIGHTS FOR PIECEWISE LINEAR FINITE ELEMENTS

$(\Delta x = d/2)$

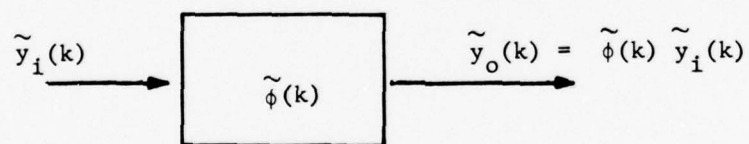| SCHEME	DENOTED	α_0	α_1	α_2	β_0	β_1	β_2	β_3	σ_1	σ_2	σ_3
A	AFE	$\frac{4}{6}$	0	$\frac{1}{6}$	$\frac{4}{6}$	0	$\frac{1}{6}$	0	0	$\frac{1}{4}$	0
B	BFE	$\frac{4}{6}$	0	$\frac{1}{6}$	$\frac{4}{6}$	0	$\frac{1}{6}$	0	$\frac{5}{16}$	0	$\frac{1}{16}$
C	CFE	$\frac{4}{6}$	0	$\frac{1}{6}$	0	$\frac{23}{48}$	0	$\frac{1}{48}$	$\frac{5}{16}$	0	$\frac{1}{16}$

LIST OF FIGURES

$$y_i(x) \longrightarrow \boxed{\phi(x)} \longrightarrow y_o(x) = \int_{-\infty}^{\infty} \phi(x-s)\, y_i(s)\, ds$$

(a) Physical Domain

$$\tilde{y}_i(k) \longrightarrow \boxed{\tilde{\phi}(k)} \longrightarrow \tilde{y}_o(k) = \tilde{\phi}(k)\, \tilde{y}_i(k)$$

(b) Transform Domain

Figure 1

Figure 2

FIGURE 3

-30-
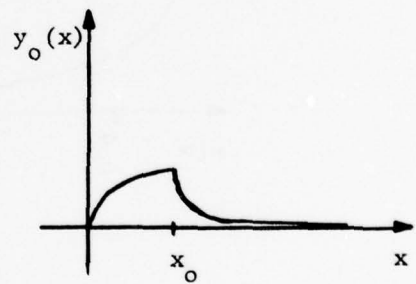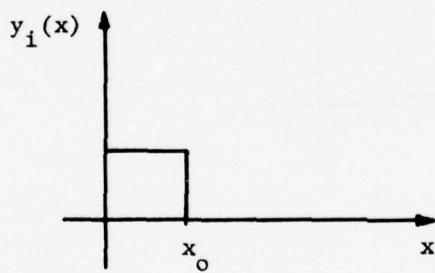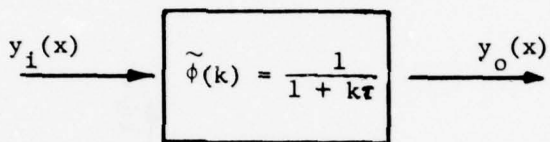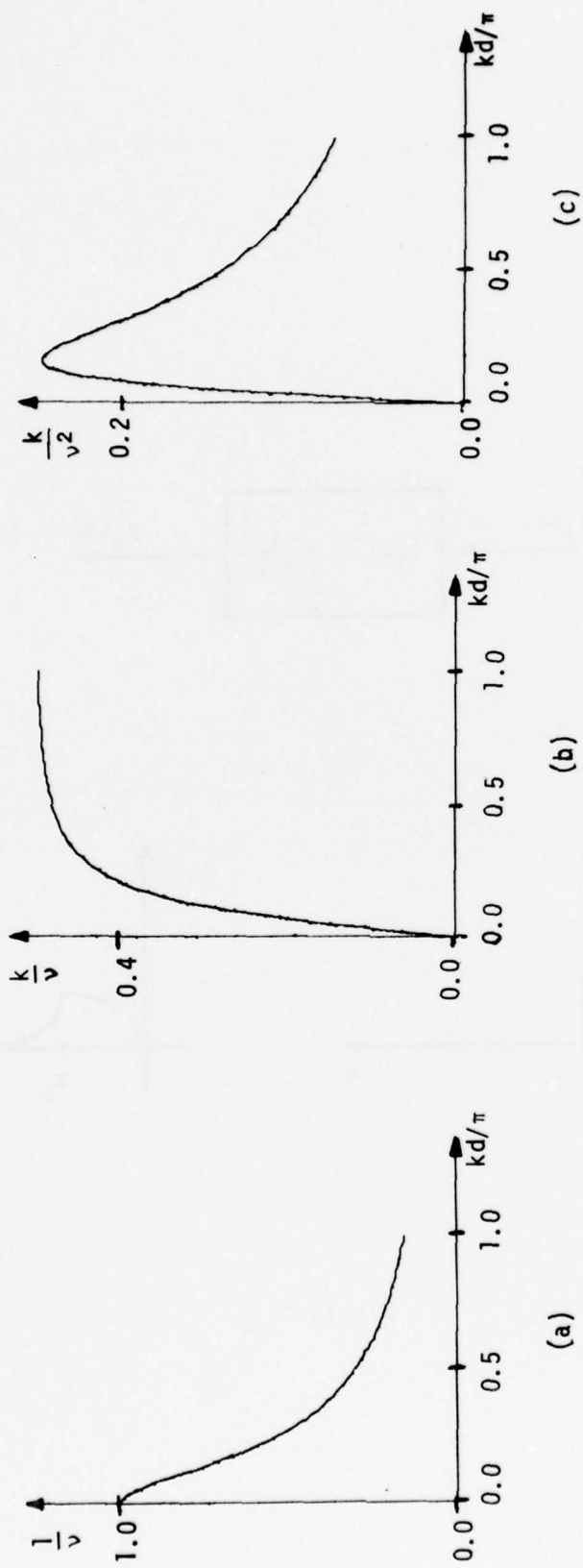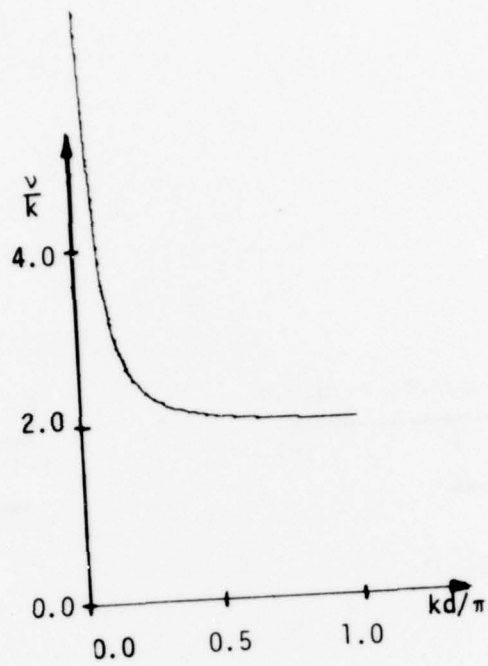
(a)
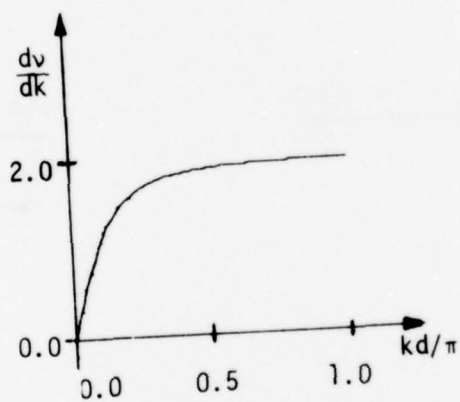
(b)
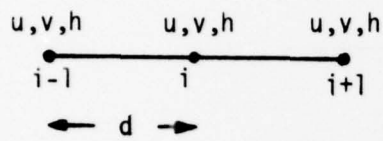
FIGURE 4

SCHEME A
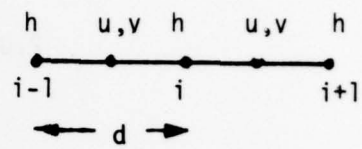
SCHEME B
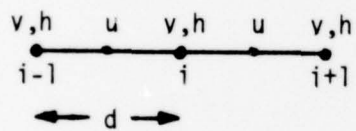
SCHEME C
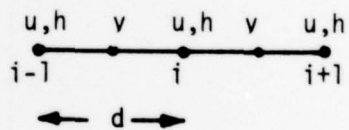
SCHEME D

FIGURE 5
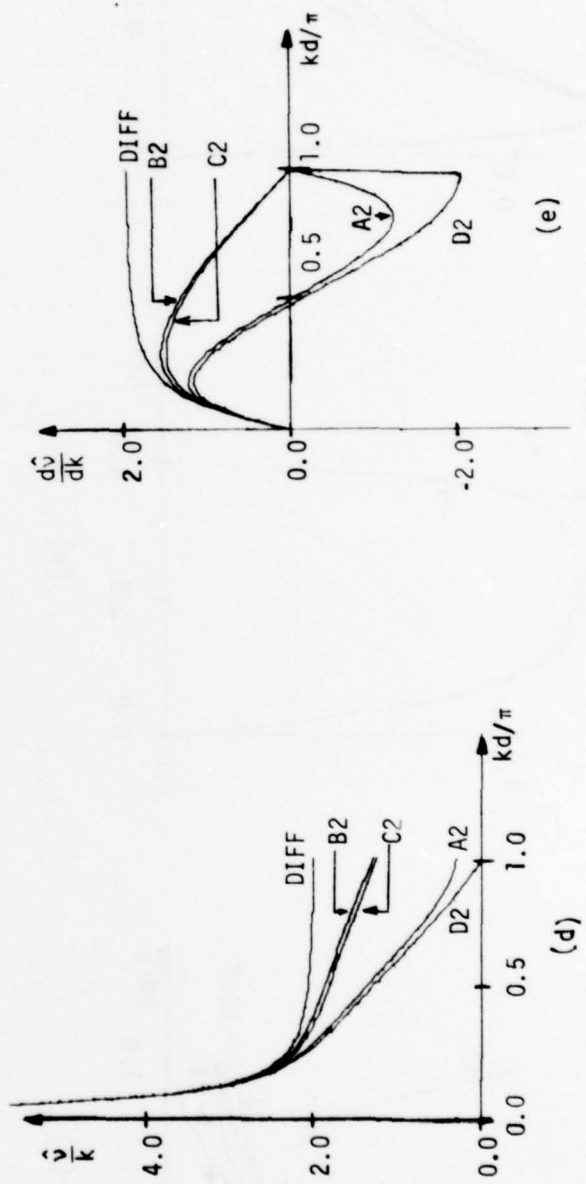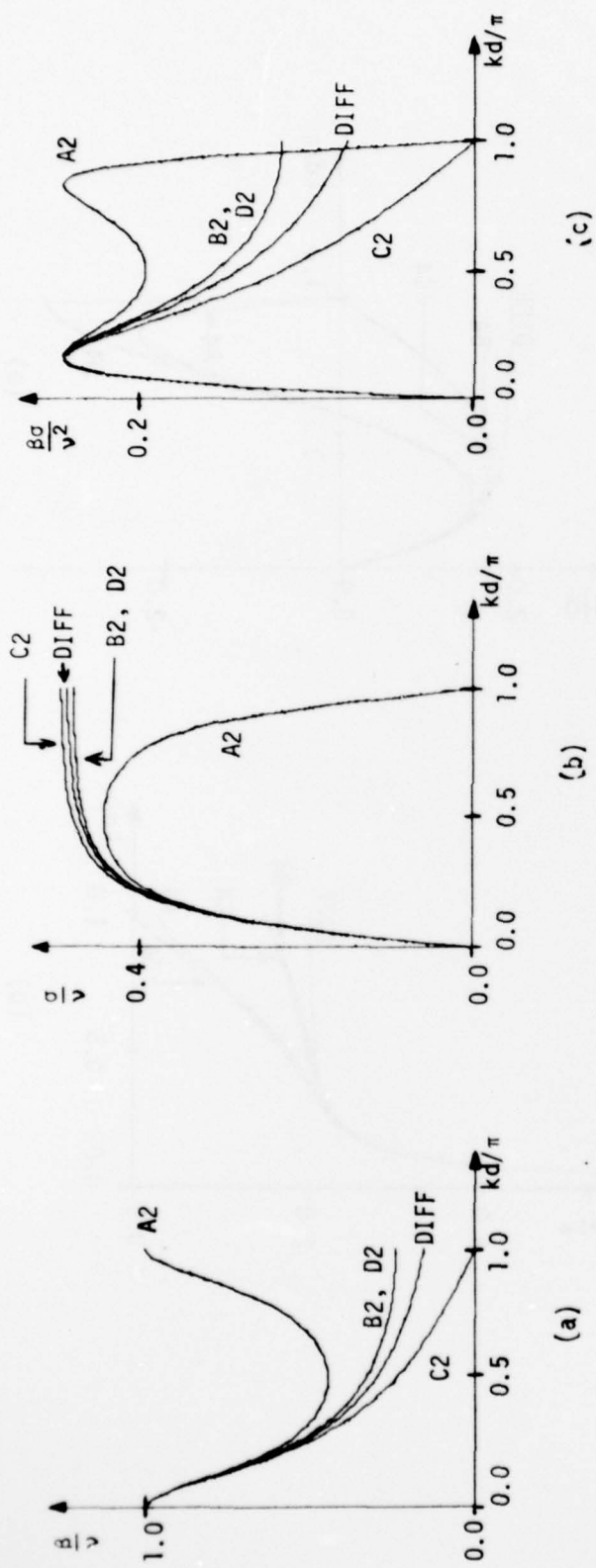
FIGURE 6

FIGURE 7

FIGURE 8

CFE

BFE

AFE

D4

C4

B4

A4

D2

C2

B2

A2

DIFFERENTIAL

8   16   24   32   40   48   56   64   (x/d)
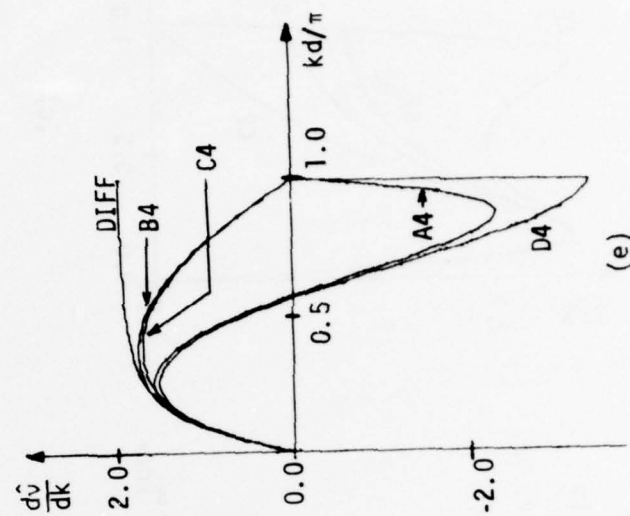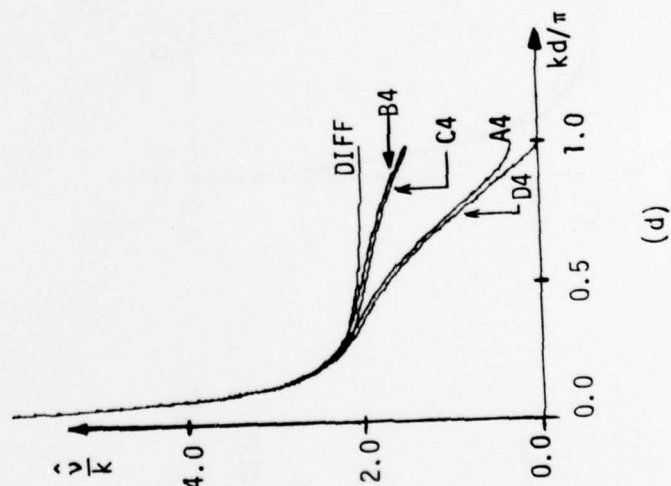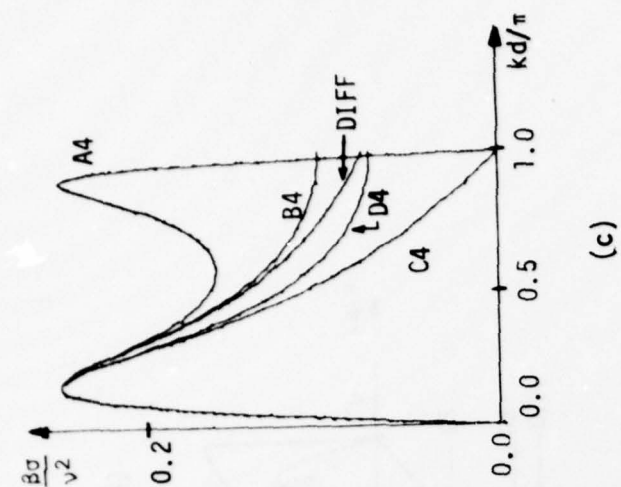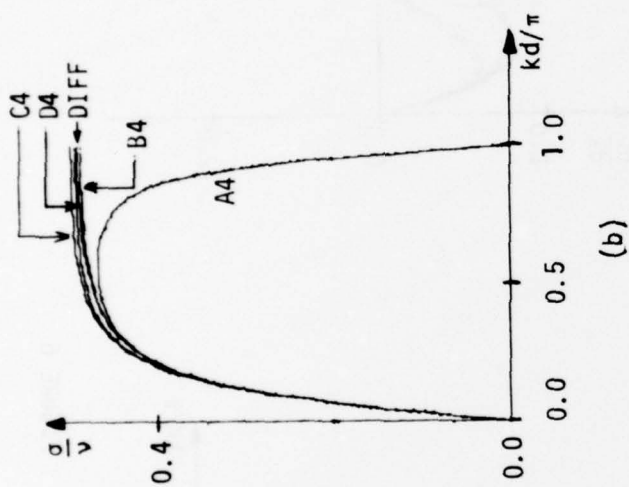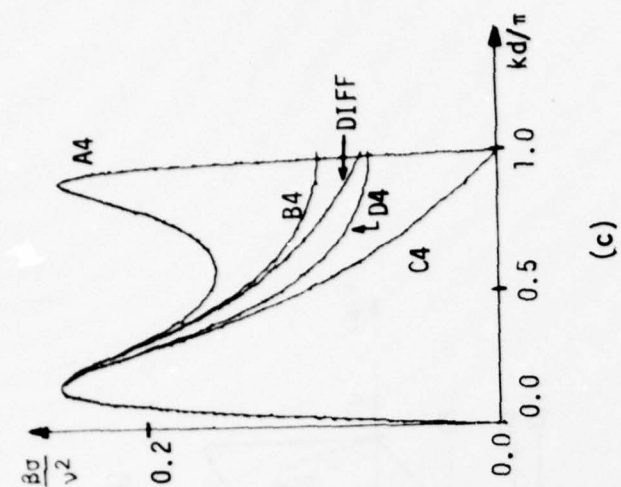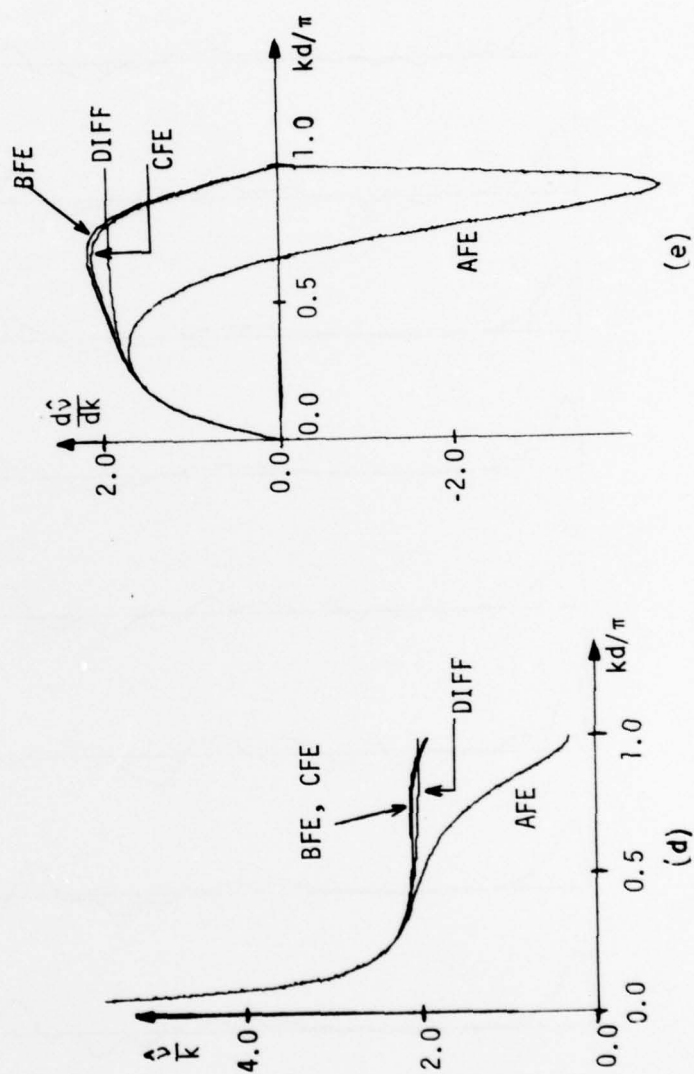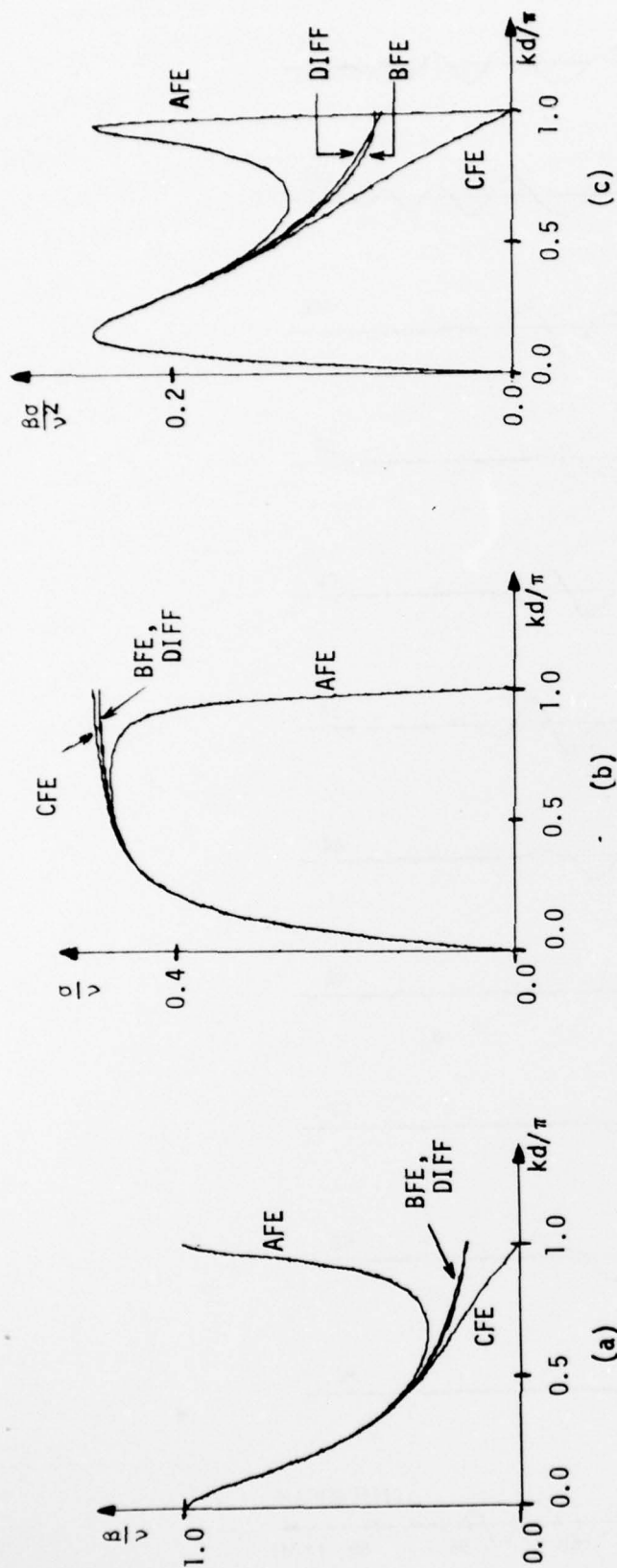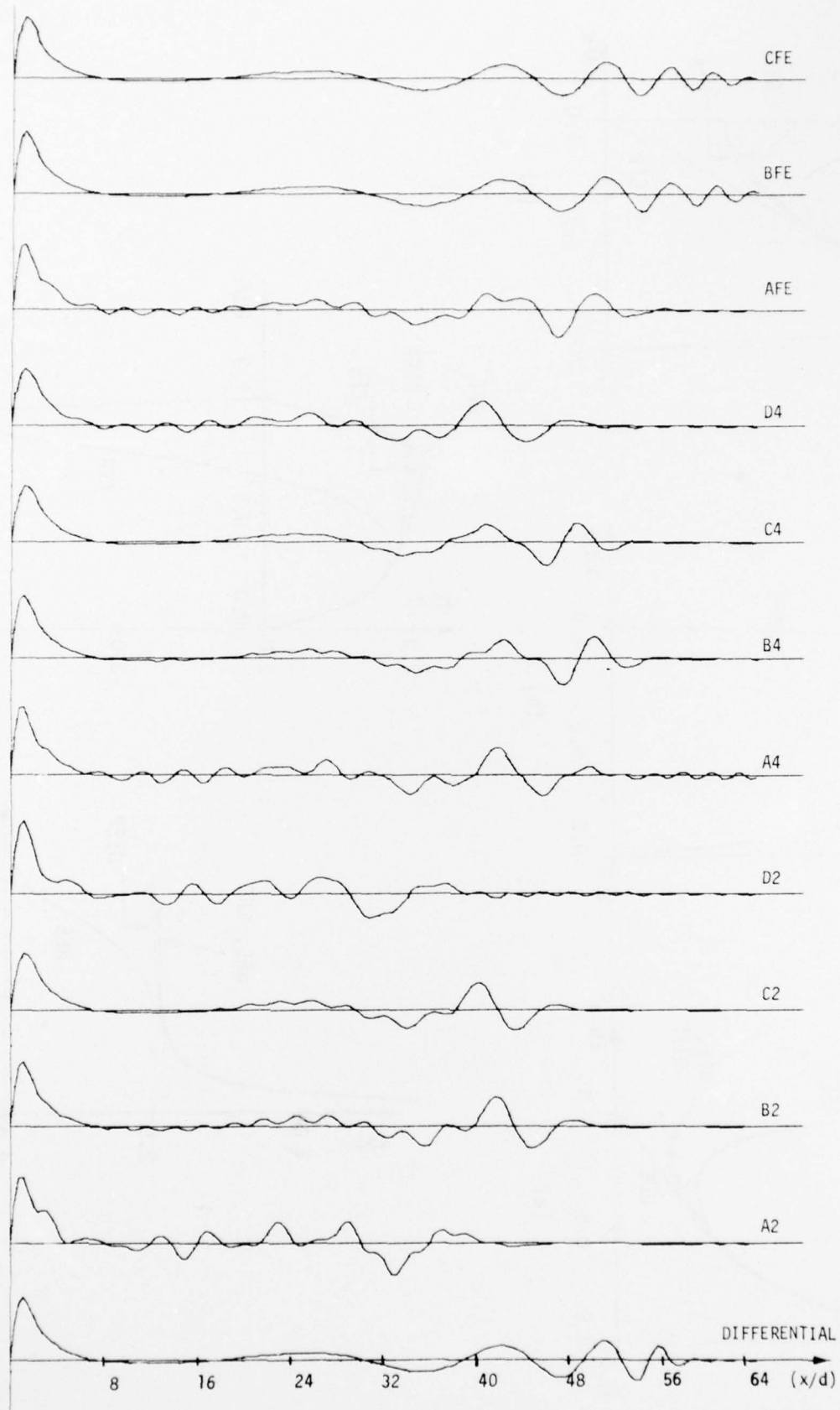
-36-

FIGURE 9

DISTRIBUTION LIST

No. Copies

1. Defense Documentation Center   2
   Cameron Station
   Alexandria, VA 22314

2. Dudley Knox Library, Code 0212   2
   Naval Postgraduate School
   Monterey, CA 93940

3. Dr. A. L. Schoenstadt, Code 53Zh   26
   Department of Mathematics
   Naval Postgraduate School
   Monterey, CA 93940

4. Dr. R. T. Williams, Code 51Wu   1
   Department of Meteorology
   Naval Postgraduate School
   Monterey, CA 93940

5. Commanding Officer   1
   Naval Weather Service Command Headquarters
   3101 Building 200
   Washington Navy Yard
   Washington, D. C. 20374

6. Officer in Charge   10
   Environmental Prediction Research Facility
   Naval Postgraduate School
   Monterey, CA 93940

7. Dean of Research, Code 012   2
   Naval Postgraduate School
   Monterey, CA 93940

8. Commanding Officer   2
   Fleet Numerical Weather Central
   Naval Postgraduate School
   Monterey, CA 93940

9. Naval Oceanographic Office   1
   Library (Code 3330)
   Washington, D. C. 20373

10. AFCRL - Research Library   1
    L. G. Hanscom Field
    ATTN: Nancy Davis/Stop 29
    Bedford, MA 01730

11. Commander, Air Weather Service   1
     Military Airlift Command
     United States Air Force
     Scott Air Force Base, IL   62226

12. Dr. R. Alexander   1
     The RAND Corporation
     1700 Main Street
     Santa Monica, CA   90406

13. Dr. A. Arakawa   1
     Department of Meteorology
     University of California
     Los Angeles, CA   90024

14. Dr. David A. Archer   1
     Douglas DuPont Rachford, Inc.
     6150 Chevy Chase
     Houston, TX   77027

15. Atmospheric Sciences Library   1
     National Oceanic and Atmospheric Administration
     Silver Spring, MD   20910

16. Mr. E. Barker   1
     Environmental Prediction Research Facility
     Naval Postgraduate School
     Monterey, CA 93940

17. Dr. Tom Beer   1
     Western Australian Institute of Technology
     Hayman Road South Bentley
     Western Australia   6102

18. Dr. W. Blumen   1
     Department of Astro-Geophysics
     University of Colorado
     Boulder, CO   80302

19. Dr. F. P. Bretherton   1
     National Center for Atmospheric Research
     P. O. Box 3000
     Boulder, CO   80303

20. Professor Dr. Jurgen Brickmann   1
     Universitat Konstanz
     Fachbereich Chemie
     775 Konstanz
     Postfach 77 33

21. Dr. John Brown   1
     National Meteorology
     Naval Postgraduate School
     Monterey, CA 93940

22. Dr. C. P. Chang, Code 51Cj   1
     Department of Meteorology
     Naval Postgraduate School
     Monterey, CA 93940

23. Professor J. G. Charney   1
     54-1424
     Massachusetts Institute of Technology
     Cambridge, MA 02139

24. Dr. Tom Delmer   1
     Science Applications, Inc.
     P. O. Box 2351
     La Jolla, CA 92037

25. Dr. D. Dietrick   1
     JAYCOR
     205 S. Whiting St., Suite 409
     Alexandria, VA 22304

26. Dr. Hugh W. Ellsaesser   1
     Lawrence Livermore Laboratory
     P. O. Box 808
     Livermore, CA 94550

27. Dr. R. L. Elsberry, Code 63Es   1
     Department of Meteorology
     Naval Postgraduate School
     Monterey, CA 93940

28. Dr. Frank D. Faulkner, Code 53Fa   1
     Department of Mathematics
     Naval Postgraduate School
     Monterey, CA 93940

29. Dr. Richard Franke, Code 53Fe   1
     Department of Mathematics
     Naval Postgraduate School
     Monterey, CA 93940

30. Dr. J. A. Galt   1
     NOAA - Pac. Mar. Envir. Lab.
     University of Washington WB-10
     Seattle, WA 98105

31. Dr. W. L. Gates   1
     The RAND Corporation
     1700 Main Street
     Santa Monica, CA 90406

32. Ian Gladwell   1
     Department of Mathematics
     University of Manchester
     Manchester M13 9PL
     ENGLAND

33.   Dr. G. J. Haltiner, Code 63Ha   1
      Chairman, Department of Meteorology
      Naval Postgraduate School
      Monterey, CA 93940

34.   Dr. R. L. Haney, Code 63Hy   1
      Department of Meteorology
      Naval Postgraduate School
      Monterey, CA 93940

35.   LT Donald Hinsman   1
      Fleet Numerical Weather Central
      Naval Postgraduate School
      Monterey, CA 93940

36.   D. Narayana Holla   1
      Department of Maths
      Indian Institute of Technology, Bombay
      P. O., I. I. T. Bombay
      Powai, Bombay 400 076 INDIA

37.   Dr. J. Holton   1
      Department of Atmospheric Sciences
      University of Washington
      Seattle, WA 98105

38.   Dr. B. J. Hoskins   1
      Department of Geophysics
      University of Reading
      Reading
      United Kingdom

39.   W. Horsthemke   1
      Universite Libre De Bruxelles-Faculte Des Sci.
      Service De Chimie Physique II-Prof. Prigogine
      C.P. 231 Campus Plaine-Bd. du Triomphe
      1050 Bruxelles - BELGIQUE

40.   Dr. D. Houghton   1
      Department of Meteorology
      University of Wisconsin
      Madison, WI 53706

41.   Dennis C. Jespersen   1
      Mathematics Research Center
      University of Wisconsin-Madison
      610 Walnut Street
      Madison, WI 53706

42.   Dr. A. Kasahara   1
      National Center for Atmospheric Research
      P. O. Box 3000
      Boulder, CO 80303

43. E. J. Kansh   1
    U.S. Department of the Interior
    Bureau of Mines
    Pittsburgh, PA 15213

44. Dr. L. D. Kovach, Code 53Kv   1
    Department of Mathematics
    Naval Postgraduate School
    Monterey, CA 93940

45. Ing. J. Kumicak   1
    Institute of Radioecology
     and Applied Nuclear Techniques
    Komenskeho 9
    P. O. Box A-41
    040 61 Kosice
    CSSR CZECHOSLOVAKIA

46. Dr. C. E. Leith   1
    National Center for Atmospheric Research
    P. O. Box 3000
    Boulder, CO 80303

47. Dr. J. M. Lewis   1
    Laboratory for Atmospheric Research
    University of Illinois
    Urbana, IL 61801

48. Mei-Kao Liu   1
    System Applications, Inc.
    950 Northgate Drive
    San Rafael, CA 94903

49. Dr. E. N. Lorenz   1
    Department of Meteorology
    Massachusetts Institute of Technology
    Cambridge, MA 02139

50. F. Ludwikow   1
    Medical School Department of Biophysics
    ul. Chalubinskiego 10
    50-368 Wroclaw
    POLAND

51. Leon Lupidus   1
    Princeton University
    School of Engineering/Applied Science
    Department of Chemical Engineering
    The Engineering Quadrangle
    Princeton, NJ 08540

52. Dr. R. Madala   1
    Code 7750
    Naval Research Laboratory
    Washington, D. C. 20390

53. Dr. J. D. Mahlman   1
    Geophysical Fluid Dynamics Laboratory
    Princeton University
    Princeton, NJ 08540

54. Dr. Alsan Meric   1
    Applied Mathematics Division
    Marmara Research Institute
    P.K. 141, Kadikoy - Istanbul
    TURKEY

55. Dr. G. Morris, Code 53Mj   1
    Department of Mathematics
    Naval Postgraduate School
    Monterey, CA 93940

56. Professor J. LL. Morris   1
    Computer Science
    University of Waterloo
    Waterloo, Ontario
    CANADA

57. Meteorology Library (Code 63)   1
    Naval Postgraduate School
    Monterey, CA 93940

58. LT W. F. Mihok   1
    Fleet Numerical Weather Central
    Naval Postgraduate School
    Monterey, CA 93940

59. National Center for Atmospheric Research   1
    Box 1470
    Boulder, CO 80302

60. Director, Naval Research Laboratory   1
    ATTN: Technical Services Information Center
    Washington, D. C. 20390

61. Department of Oceanography, Code 68   1
    Naval Postgraduate School
    Monterey, CA 93940

62. Office of Naval Research   1
    Department of the Navy
    Washington, D. C. 20360

63. Dr. T. Ogura
    Laboratory for Atmospheric Research
    University of Illinois
    Urbana, IL 61801   1

64. Darrell W. Pepper   1
    Environ. Transport Div.
    E.I. du Pont de Nemours & Co., Inc.
    Savannah River Laboratory
    Aiken, SC 29801

65. Professor N. A. Phillips   1
    National Meteorologican Center/NOAA
    World Weather Building
    Washington, D. C. 20233

66. Dr. S. Piacsek   1
    Code 7750
    Naval Research Laboratory
    Washington, D. C. 20390

67. A. P. Raiche   1
    Minerals Research Laboratories, C.S.I.R.O.
    P. O. Box 136
    North Ryde, N.S.W. 2113
    AUSTRALIA

68. Dr. T. Rosmond   1
    Environmental Prediction Research Facility
    Naval Postgraduate School
    Monterey, CA 93940

69. Dr. Y. Sasaki   1
    Department of Meteorology
    University of Oklahoma
    Norman, OK 73069

70. Dr. Fred Shuman, Director   1
    National Meteorological Center
    World Weather Building
    Washington, D. C. 20233

71. Dr. R. Somerville   1
    NCAR
    P. O. Box 3000
    Boulder, CO 80303

72. Dr. Mevlüt Teymur   1
    Applied Mathematics Division
    Marmara Research Institute
    P.K. 141, Kadikoy - Istanbul
    TURKEY

73. Dr. D. Williamson   1
    National Center for Atmospheric Research
    P. O. Box 3000
    Boulder, CO 80303

74. Professor Carroll O. Wilde   1
    Chairman, Department of Mathematics
    Naval Postgraduate School
    Monterey, CA 93940

75. Dr. F. J. Winninghoff   1
    1085 Steeles Avenue, #503
    Willowdale (Toronto)
    Ontario M2R2Tl CANADA

76. Dr. M. G. Wurtele   1
    Department of Meteorology
    University of California
    Los Angeles, CA 90024

77. Dr. J. Young   1
    Department of Meteorology
    University of Wisconsin
    Madison, WI 53706